

# Resource-Centric Serverless Computing

Zhiyuan Guo   Zachary Blanco   Mohammad Shahrada\*   Zerui Wei  
Bili Dong   Jinmou Li   Ishaan Pota§   Harry Xu§   Yiying Zhang  
*UC San Diego*   \**University of British Columbia*   §*UC Los Angeles*

## Abstract

Today’s serverless computing has several key limitations including per-function resource limits, fixed CPU-to-memory ratio, and constant resource allocation throughout a function execution and across different invocations of it. The root cause of these limitations is the “function-centric” model: a function is a fixed-size box that is allocated, executed, and terminated as an inseparable unit. This unit is pre-defined by the cloud provider and cannot properly capture user needs.

We propose a “resource-centric” model for serverless computing, which adapts the underlying provider serverless systems to follow applications’ natural resource needs. To achieve this vision, we built Scad based on two ideas: disaggregating a serverless application based on its resource features and aggregating disaggregated units for better performance. Our results show that Scad solves various resource-related issues of today’s serverless computing, while retaining or even improving its performance.

## 1 Introduction

Serverless computing, commonly offered in the form of Function-as-a-Service (FaaS), is a type of cloud service that allows users to deploy and execute their applications without managing servers. Serverless computing has gained significant popularity in recent years because of its benefits to cloud users: minimal IT burdens and paying only when their applications run.

Despite many benefits, today’s FaaS-based serverless computing still has several key limitations. First, there are few fixed CPU-to-memory ratios that users can choose, while workloads can have arbitrary CPU-to-memory ratios. As a result, either some CPU or memory is wasted [17]. Second, a function’s resource reservation is fixed across invocations, but different inputs to the same function could result in different resource requirements [17]. This lack of elasticity would result in resource waste or in the worst case, function failure, if an invocation exceeds the resource reservation. Third, all resources are allocated from the provider at the beginning of a function and deallocated at the end of it. Thus, users have to provision functions for peak usages but end up not using the peak resources all the time. Meanwhile, data generated during

function execution cannot live after execution ends, which makes sharing such data across functions harder [37, 56]. Finally, the amount of resources a function can use is limited, which can force users to rewrite their large-scale applications like data analytics as smaller pieces that can fit in functions.

Our observation is that the root cause of these limitations is today’s *function-centric* serverless model. A function is a rigid, fixed-size box that couples CPU and memory resources and is allocated, scheduled, terminated, and billed as an inseparable unit. Different functions belonging to the same application are separated from each other over slow communication methods. This function-based model leaves users with a dilemma: either pack more functionality into a large function to avoid communication cost but pay for unused resources during non-peak portion of execution, or split functionality into fine-grained functions to more precisely provision each function’s resource but incur high function-communication performance overhead. Moreover, neither option is always possible, since even the largest function sizes will not be able to host arbitrarily large applications in their entirety, and certain applications cannot be properly split into small pieces as a task flow.

Crucially, fixed-size resource allocations are predefined by the cloud providers and cannot properly capture user application behavior. Instead of having users (re-)structure their applications to follow provider-defined boxes, we believe that providers should execute applications by following applications’ own structure and resource needs. Driven by this insight, we propose to center serverless computing around the *resource features* of applications, which we call *resource-centric serverless computing*. To enable this vision, we judiciously exploit two ideas, *disaggregation* and *aggregation*.

**Disaggregation.** Our first idea is based on resource disaggregation, a popular data-center architecture which separates resources into different pools. Today’s disaggregation systems disaggregate user applications based on their resource types (*e.g.*, separating compute from memory) [50, 52, 62]. To fit the elasticity of serverless computing, we propose to also disaggregate based on (1) resource amount and (2) span of execution (*i.e.*, phases or relative time windows within an application’s execution time). Specifically, we disaggregate

a serverless application into *components*, each representing either a piece of application code (*i.e.*, compute component) or a data structure (*i.e.*, memory component) with a distinct triad,  $\langle \text{resource type, resource amount, span} \rangle$ . Components with different resource types run on different disaggregated resource pools. A user application can be described as a *component graph*, where one component can communicate with or trigger other ones.

Serverless-specific disaggregation has several key benefits. First, it enables the independent scaling of different resource types, thereby allowing arbitrary resource ratios (*e.g.*, CPU-to-memory ratio). Second, instead of provisioning for the peak resource usage, we can use multiple components to capture resource consumption changes in a user application. Third, when pooling resources, applications can allocate and use resources beyond what a single node can provide. Finally, when serverless applications want to access or share data that cannot fit into the local environment, allowing them to use a memory interface to access disaggregated memory could potentially yield better performance than accessing a storage layer via a storage interface as in today’s serverless systems. Together, the first two features improve *resource efficiency*, and the latter two improve *performance*.

**Aggregation.** Despite its benefits, disaggregation inevitably incurs increased network communication. Moreover, when disaggregating an application into smaller units, each of them could potentially incur scheduling and startup overhead. To reduce or eliminate these overheads, our second idea is to merge, or *aggregate*, components and when possible, run them together in a *balanced pool*, where each server is equipped with similar amounts of CPU and memory resources. Aggregated components can run locally in one environment on one server, avoiding the network communication overhead, startup time, and scheduling burden.

**Scad.** We built *Scad (Serverless Computing with Aggregation and Disaggregation)*, a resource-centric serverless computing framework that dynamically aggregates and disaggregates components based on resource utilization and application behavior. Users can port their applications to Scad by annotating the original programs or by using libraries that Scad provides. Under the hood, our compiler and libraries map user applications to a component-based interface that Scad executes. Scad can run all applications supported by today’s serverless platforms and many that are not. Applications whose resource usage patterns vary during the execution and/or use vast amounts of resources can especially benefit from Scad.

Despite these many benefits, disaggregation and aggregation in a serverless setting bring two major challenges.

First, *how to deal with dynamic resource scaling and aggregation that components must undertake* at the run time to achieve our targeted performance and resource benefits. For instance, a memory component may contain an array that grows dynamically, possibly requiring space beyond what the server that hosts it can offer. As another example, Scad may

need to aggregate a compute and a memory component to improve their communication performance. To enable flexible resource adjustment, we decouple *virtual* and *physical* components. Virtual components, which capture application features and are generated statically by compilers, remain unchanged throughout the execution. Physical components, on the contrary, are dynamically added, released, or merged at run time in response to load changes. As a result, there can be one-to-one, one-to-many, or many-to-one relationships between virtual and physical components. These relationships are managed dynamically by Scad, enabling elasticity in a straightforward manner.

Second, *how to efficiently handle the two relationships in component graphs: data communication and task triggering*. Different from traditional disaggregation systems which focus on optimizing the run-time communication performance (data plane), in a serverless setting, we also need to efficiently start up the communication across *dynamically instantiated* components (control plane). We build an RDMA-based communication system that judiciously exploits an indirect channel for connection setup, while allowing direct component-to-component communication after the setup. Different from today’s serverless task-flow systems, our component graph can contain many more components, demanding efficient scheduling and failure handling. We propose a two-level scheduling system that launches components in a just-in-time, asynchronous, and reliable manner.

We implemented Scad on top of OpenWhisk [4] and evaluated it with a set of microbenchmarks and two real-world applications: machine-learning training and data analytics with a TPC-DS benchmark. We compared Scad to OpenWhisk, AWS Lambda, AWS Step Functions [5], Azure Durable Functions [6, 18], and PyWren [34]. Our application-level results demonstrate that Scad reduces the memory footprint of up to  $1.96\times$  while improving total application execution time by up to 28% compared to existing systems.

## 2 Motivation, Challenges, and Related Work

This section discusses the limitations of today’s serverless computing, summarizes related works, and presents new challenges which motivate Scad.

### 2.1 Today’s Serverless Computing

Despite its wide adoption, there are still many limitations that prevent (or delay) serverless computing’s wider adoption.

**Lack of elasticity and fixed resource ratio.** Today’s serverless functions have limited scale-up capabilities. If a function tries to use more memory than what is given by the provider (*e.g.*, a fixed max of 1.5 GB with Azure Functions’ Consumption Plan), it will be aborted. Additionally, the majority of serverless offerings come with fixed compute-to-memory ratios. For example, AWS Lambda uses a fixed ratio of vCPUs to memory (1 vCPU for up to 1,769 MB) [38]. Fixed ratios cannot cover what most applications need [17]. Moreover, the

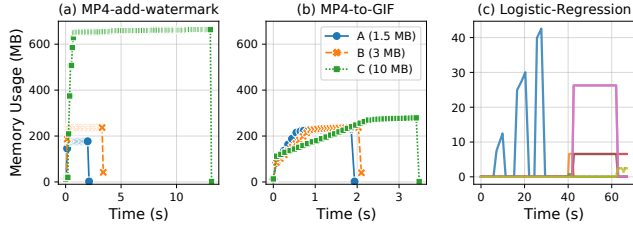


Figure 1: **Memory Usage Examples.** (a) (b) are two stages in a video processing application [21] with three input videos. (c) shows memory consumption of major data structures in a Logistic Regression application [19].

same application’s CPU-memory consumption ratio could vary with different inputs [27, 41]. This leaves users paying higher prices, and cloud providers with underutilized infrastructure.

Figure 1 shows the memory usage of two stages in a video processing application (from [21]). The first stage downloads an MP4 video file and adds a watermark to it. The second stage exports this new MP4 to the GIF format. We invoke this chain with inputs as URLs to three 30-second-long videos. Due to different video qualities, the corresponding video files are 1.5, 3, and 10 megabytes in size. We run the application in a docker container with 4 vCPUs. As Figure 1(a)(b) shows, for different inputs, the watermark stage uses different amounts of memory for the same vCPUs, while the GIF stage’s memory-to-core ratio does not change with inputs. Moreover, these two stages belong to the same application but their memory-to-core ratios can differ a lot.

While we used this serverless application to demonstrate the resource ratio mismatch, this problem is quite prevalent. A recent study showed that intelligently choosing a configuration from 48 different CPU-memory combinations can already reduce serverless workloads’ execution costs by up to 50% [17]. This study assumes that the chosen CPU-memory combinations can always be scheduled. However, in reality, allowing containers to have more CPU-memory ratios makes scheduling harder, as the scheduling algorithm must perform multi-dimensional bin-packing to fit containers to servers. Moreover, even if arbitrary CPU-memory ratio could be scheduled, one single ratio may not always be ideal for the entire duration of a function.

*Insight 1: A more viable solution to the CPU-memory ratio problem is not to offer more ratios but to eliminate fixed ratios altogether, by decoupling CPU and memory as separate allocation and scheduling units.*

**Coarse-grained, coupled resource time span.** All resources for a function in today’s serverless platforms have the same time span, as they are allocated in the beginning and released at the end of a function’s execution (or beyond a function’s execution to keep it alive for faster future invocation). This results in resource waste for providers and/or extra costs for users, since a function can often have different phases of resource usages during execution.

For example, Figure 1(c) shows the memory consumption of several large data structures in a logistic regression program [19] over time. Clearly, this application has different phases of memory consumption.

It is possible to change the billing model to charge for only what is used. For instance, Azure Functions charges based on dynamic memory usage by rounding up to the nearest 128 MB [7]. However, the cloud provider is still left with the incurred cost for the unused resources since all resources are still allocated for the whole function duration [51].

Today’s serverless model makes it hard to decouple data’s time span from function execution, as the primary way to maintain data after a function ends is to write it to another data-store layer like S3. Several recent research works aim to address this problem by maintaining function results (intermediate data) in a fast, specialized data store [37, 41, 46, 48, 56, 61]. One common limitation of these works is the coarse-grained approach they take: a function’s intermediate data is often read/written as an object at the beginning/end of the function. This requires the entire intermediate data to live both with the function and at the intermediate data storage layer for the entire period of the function, doubling the memory resource consumption, as we will show in §5.2.

*Insight 2: Decoupling resources with different time spans can reduce the overall resource consumption.*

**Per-function resource limits.** All serverless providers set a limit for the maximum resource consumption of a function. For example, Azure Functions’ Consumption Plan limits application memory to 1.5 GB [7]. Resource limits significantly complicate deploying medium- to large-scale applications such as data analytics [34] and DNN training [66]. The current workaround for hard resource limits is to rewrite user applications by splitting them into smaller pieces each of which fits in a function’s quota [34, 46, 67]. Rewriting applications not only adds developer burden but could also lead to new performance issues because of the slow function-to-function communication. There is no fundamental reason why a function’s quota cannot be increased and it has. For instance, AWS Lambda increased the per-function memory limit from 3,008 MB to 10,240 MB in December 2020, which soon enabled new applications [1, 2]. However, larger functions could result in more resource wastage because not the entire execution would need to use the allocated resources. Larger functions are also harder for providers to schedule.

*Insight 3: Instead of continuing to increase function resource limits, it is more desirable to not impose any limits<sup>1</sup> and do so without making resource allocation harder.*

<sup>1</sup>Scad users can specify a maximum resource limit across all invocations of their applications to prevent malicious or unintentional surge in cost.

## 2.2 Resource Disaggregation

Resource disaggregation is an increasingly popular data-center architecture that organizes different hardware resources into separate, network-attached pools. Resource disaggregation can either be physical, where devices or dedicated servers are physically separated by the network [12, 15, 32, 52, 59], or virtual, where different resources are physically co-located in the same servers but are virtually managed separately [24, 35, 42]. Scad works for both cases.

Disaggregation could potentially solve various resource-related issues of FaaS, as discussed in §1. At the same time, serverless computing could be one killer application for resource disaggregation systems, as its elastic and fine-grained features naturally fit disaggregated architectures [11, 30, 44].

Disaggregation in the serverless setting has several new demands and challenges. First, serverless computing demand new disaggregation criteria. For example, in addition to resource type, serverless systems can also benefit from disaggregating according to resource amount and/or time span. Second, a disaggregated unit should be elastic and auto-scaled on demand at the run time, as resource demands vary across different inputs and are hard to predict. Third, the launch and scheduling of disaggregated units should be efficient. Unlike today’s disaggregated memory systems that pre-allocate remote memory, in a serverless setting such pre-allocation would cause resource wastage. Finally, the communication across disaggregated units can be heavy and affect application performance. Today’s function-to-function communication is not designed for such frequent communication and would be too slow for disaggregated units. Existing disaggregation solutions enable fast communication but assume that disaggregated units’ locations are pre-defined and known to each other, which does not meet serverless’ elasticity requirements.

## 2.3 Resource Aggregation

We are the first to propose aggregating disaggregated units in an application. A related idea in the serverless world is to *co-locate* several functions. SAND [14] proposes to merge function chains into a single container image. Photons [26] and FAASM [53] explored the co-location of concurrent invocations of the same function. These solutions co-locate functions to mainly reduce cold start cost. Scad aggregates resource-based components mainly to improve the execution time of an application (by avoiding frequent network communication). Scad’s aggregation approach raises at least two new challenges. First, there can be many ways to aggregate different combinations of components in a complex component graph. Second, because Scad may still disaggregate aggregated components at a later time, we need to keep monitoring the interaction among already aggregated components.

## 3 Scad Abstractions

This section introduces Scad’s two-level abstractions. Currently, Scad supports programs written in Python, the most

commonly used programming language in serverless [23].

### 3.1 Resource-Based View of Applications

Different from FaaS-based serverless, Scad’s view of a serverless application is based on its resource features. Scad views applications as *resource-based components*, or simply, *components*. A component encapsulates a part of an application that has the same or similar resource features (*i.e.*, same *type* of resources with similar *amounts* that are active over the same time *span* in the execution flow). Currently, we support two components: a *compute component* which contains a piece of code with a single entry point and *memory component* which contains in-memory data structures. Scad places a compute component in the compute pool when its local memory usage is small; when its memory usage grows, Scad moves it to the balanced pool. Scad places all memory components in the memory pool.

Components can have two relationships: 1) a compute component can trigger one or more compute components and send its output to them, what we call the *triggering relationship*, and 2) a compute component can access data in memory components and exchange messages with other compute components, what we call the *communicating relationship*. Note that different from compute components, memory components are not explicitly triggered. Instead, Scad automatically starts a memory component when a compute component first initiates the access to it. It ends when the last compute component accessing it ends or explicitly releases it.

Components in an application form a *component graph*, with components as vertices and component relationships as edges. A component graph is what sits between the user application and Scad’s execution. A user application can be statically mapped to a component graph either by compilers or expert developers (§3.2), and Scad generates execution units based on the component graph at run time (to be discussed in §3.3).

### 3.2 Scad Programming Models

Scad provides two layers of interfaces: a high-level interface for application developers and a low-level interface for library/runtime/compiler developers. Figure 2 illustrates these two interfaces with code snippets from a simple example.

**Low-level interface.** The low-level interface is fed to Scad’s execution system. Thus, we design it in such a way to express explicit component graphs and interactions between components. With this intermediate representation, Scad’s execution system does not need to directly analyze high-level language or application features. This interface is intended to be used as compiler output or by library and runtime developers. Specifically, the interface is described by a JSON template that specifies compute and memory components and the relationships between them in an application (*i.e.*, one JSON file represents one component graph). Each compute component points to a code piece that is submitted to Scad

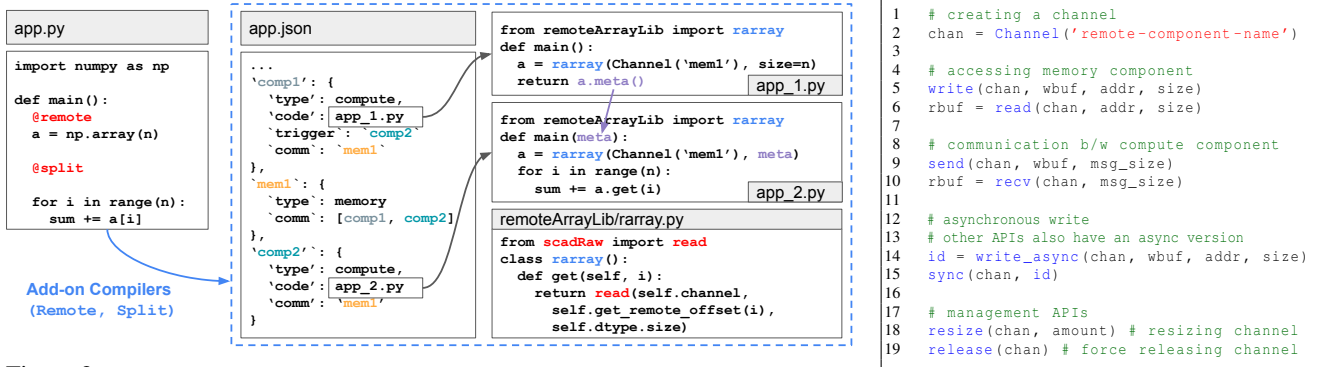


Figure 2: Scad Application Example using Scad High-Level APIs Example code of an application built with Scad high-level interfaces compiled to Scad low level interfaces.

Figure 3: Scad’s Low-Level APIs.

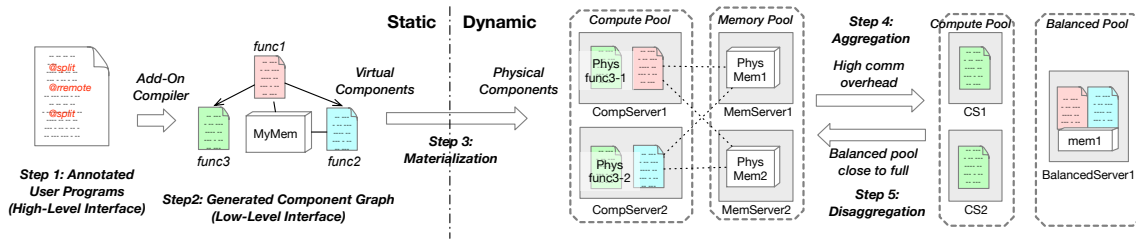


Figure 4: Scad Workflow. This example demonstrates the workflow of Scad. The user annotates her program with one remote and two split annotations. The Scad compiler then generates a graph of virtual components. At the run time, Scad materializes the virtual memory component as two physical memory components on two memory servers, two instances of `func3` and single instances of `func1` and `func2` on two compute servers. At a later time, Scad could decide to aggregate `func1`, `func2`, and `MyMem` and run them on a balanced server. At yet another time, Scad could decide to re-disaggregate the components.

together with the JSON file. This interface also includes a set of Scad low-level APIs that a compute component code can use to access other memory components or communicate with other compute components, as shown in Figure 3.

**High-level interface.** We do not expect application developers to directly use the low-level interface. Instead, we provide a high-level interface that allows developers to retain their programs’ original structure. Users just need to add simple annotations to their code or replace the original library calls to Scad’s corresponding library calls. We then compile the user code to Scad’s low-level interface and/or let Scad libraries use the low-level interface to implement library calls. As this work focuses on system-level designs, our current compiler and library serve as proof of concept. Future library and compiler developers could support richer features.

Currently, we support two annotations, `@split` and `@remote`, and two libraries.

The `split` compiler splits user code at each `@split` annotation into triggering compute components. It finds the variables that are shared across a `@split` annotation and puts them in a memory component that has communicating relationship with compute components generated from this `@split`. The compiler also converts the original accesses of these shared variables into Scad’s low-level APIs.

The `remote` compiler works with a `NumPy array` library to convert a NumPy array that is annotated with `@remote` into

a memory component. The library implements NumPy array operations with Scad’s low-level APIs.

Finally, we implemented a `DataFrame` compiler and library which can convert programs written with pandas [65] to a component graph without user annotations. It generates one compute component for each operator such as `map`, `join`, `shuffle`, and `reduce`. We also apply an optimization to generate one compute component from multiple operators of the same nature (e.g., multiple filters working on the same data). The compiler generates one memory component per `DataFrame` that a compute component accesses. The library implements each `DataFrame` operator using Scad’s low-level APIs. This compiler-library combination demonstrates the possibility of transparently porting programs that are well encapsulated into computation stages.

**Application porting.** Application developers can leverage their understanding of an application to add annotations or use Scad library calls. Our existing high-level APIs support a wide range of programs, though new compiler and libraries could be built to further decrease the effort required to port an application. For example, existing serverless programs with stages, such as a video processing pipeline may include a decompression, a pre-processing, and a face-detection phase. Each phase could process and generate a distinct data structure (e.g., a set of frames). Those stages and data structures with distinct resource requirements can be identified as com-

ponents leveraging our annotations. Application developers can also analyze their applications using profilers like Scalene [9], pprofile [8], or Memray [10] to capture how resource consumption changes and annotate their code accordingly. Future tools and compilers could potentially automate the above steps.

We released Scad in a classroom setting of 21 students with the goal of porting applications such as image inference processing [60], video processing [21], machine learning training, and data analytics [47] to Scad. All teams managed to port their applications to Scad within one day (after being able to set up OpenWhisk and understand Scad) and with less than 200 lines of code/annotation changes.

### 3.3 Component Materialization

To make Scad’s execution of user applications flexible, we map the application-facing abstraction to another internal abstraction, a process we call *materialization*. Figure 4 illustrates the workflow of Scad with a simple example. The components in the low-level-interface component graph as defined in §3.1 are *virtual*; they are intended for capturing application resource features at static time (*i.e.*, compiler-generated Scad APIs only deal with virtual components). Scad materializes them to *physical* components at the run time in a way that is optimized for run-time scheduling and execution.

A virtual component could be materialized as multiple physical components potentially on different servers. Physical components can also be dynamically added to *scale up* a virtual component. Meanwhile, multiple virtual components could be aggregated and executed as one physical component. Scad transparently maps an access of a virtual component to one or more accesses of the corresponding physical component(s). Decoupling virtual components from physical components allows Scad’s runtime to 1) transparently and dynamically *scale* a virtual components without the need to change statically generated Scad APIs, 2) allow a virtual component’s *size* to go beyond what a single machine can hold (a current FaaS limitation), 3) transparently *aggregate* multiple virtual components to avoid network communication, and 4) transparently *disaggregate* an aggregated component when resources in the balanced pool is scarce.

## 4 Scad System Design

This section presents Scad’ system design. Figure 5 illustrates the overall architecture of Scad. A Scad cluster consists of one or more racks of nodes that are organized as *resource pools*. Scad supports different resource disaggregation implementations. For example, resource pools could be physically separated where each node in a pool only serves one resource type (Node 1 and Node 3 in Figure 5 only serve for the compute and the memory pool respectively). Resource pools could also be virtual, in that one node can be part of multiple (virtual) pools, *e.g.*, Node 4 is in a virtual compute pool and a virtual memory pool. Different from traditional resource dis-

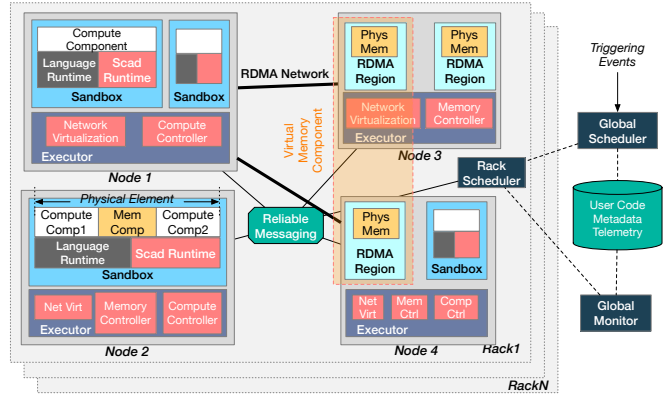


Figure 5: Scad System Architecture.

aggregation architectures, Scad also includes a *balanced pool*. Nodes in this pool (*e.g.*, Node 2) have a balance of CPU and memory.

Scad consists of three subsystems, a scheduling system, a runtime execution system, and a component adjustment system. The rest of this section will introduce each of them in the order that an application reaches it while executing.

### 4.1 Component Scheduling

After compiling, users deploy their application to Scad by submitting the generated JSON file and code pieces. The user also specifies the events which trigger the application. When such an event happens, the first component to be involved is the scheduler. Scad adopts a two-level mechanism where a *global scheduler* performs coarse-grained load balancing across racks, and each *rack-level scheduler* performs fine-grained scheduling to map physical components to nodes in the rack. This architecture enables Scad to handle scheduling requests at a high rate and fits our locality-aware scheduling policy to be discussed in §4.1.1.

Overall, the Scad scheduling system has two goals: 1) scheduling *policies* that enable efficient execution of components, and 2) scheduling *mechanisms* that enable faster startup time and to handle a large number of scheduling requests. Figure 6 plots a startup timeline with three dummy components, and latency of different steps collected when running Scad. It highlights the mechanism and efficiency of the Scad scheduling system.

#### 4.1.1 Scheduling Policy

Our scheduling policy considers two goals: communicating components should be placed close to each other in network distance to achieve better performance, and components of a specific type should go to their corresponding resource pool. Thus, our scheduling is *locality-aware* and *resource-pool aware*, in addition to traditional *warm-start awareness*.

Our policy takes the following steps when scheduling a physical component in an application: 1) For the first component in an application graph, we choose a server based on the hash of the application’s and the component’s unique ID to

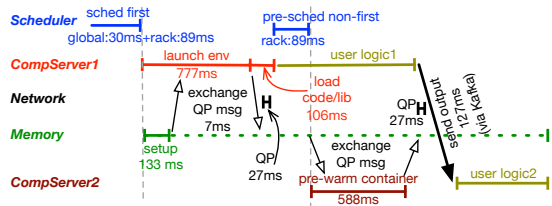


Figure 6: **Scad Startup Flow with Real Results.** This example application has two compute components and one memory component, which is shared by the compute components. Initially, Scad schedules the first compute and the memory components. They then start their own launch process in parallel. Once the environment is ready, each of them sends QP-info message to the other, after which RDMA QP can be established. At a later time, Scad pre-warms the environment for the second compute component. Dashed green line represents how long the memory component lives.

increase the probability of warm start, similar to OpenWhisk (*warm-start aware*); 2) We schedule other non-first components in the same rack as previous components that trigger them unless this rack is out of resources, in which case another lightly loaded rack is chosen (*rack-level locality*); 3) If a non-first component has other communicating component(s) that are already running, we schedule it on the same server as one of these other components if the server’s resource permits (*server-level locality*); 4) For compute components, if (3) is not possible or if there is no communicating components, we use the warm-start-aware approach in (1) to pick a server; and 5) For compute components that cannot find a hash-based server that has enough resource in (3) or for memory components, we choose a random server that has enough resources in the corresponding resource pool (*resource-pool aware*). As will be seen in §4.2.1, memory components have no application-specific environments and can just be launched on arbitrary servers in the memory pool.

#### 4.1.2 Startup-Time Optimizations

An application on Scad could involve more components than traditional FaaS functions, which means it is even more critical to start every component quickly.

##### Improving cold start time with just-in-time pre-warming.

A common way to reduce cold starts is to keep the execution environment alive after a function finishes for future invocations of it [28, 49, 51]. A complementary approach is to *pre-warm* a function based on historical invocation patterns [49, 51, 55]. State-of-the-art workflow or graph-based serverless frameworks [39, 55] treat each function in a workflow in its isolation and apply some of the pre-warm/keep-alive mechanisms. We adopt keep-alive and pre-warming for avoiding cold starts for the *first* compute component in a component graph. For non-first components, we propose a pre-warming mechanism that leverages workflow information to avoid unnecessary resource wastes to keep them alive.

Specifically, after a configurable amount of time ( $\tau$ ) since

the start of a compute component, the compute controller sends a request to the rack-level scheduler to initialize *subsequent component(s)* that this component will trigger. For each subsequent component, the scheduler finds a warm worker or starts a new sandbox to warm it up. The value  $\tau$  controls the tradeoff between visible start-up time overhead and resource wastage. If we start a subsequent component too early (*i.e.*,  $\tau$  being too small), that component’s environment will sit idle and waste resource. If we start a subsequent component too late (*i.e.*,  $\tau$  being too large), it will not be ready when the current component finishes. Ideally,  $\tau$  should be set as the total execution time of the current component minus the startup time for the subsequent component. We currently set  $\tau$  statically (*e.g.*, 0 in our experiments). Future work can use a more intelligent way to set it (*e.g.*, by predicting the execution time of a component).

**Improving warm start time.** While most serverless systems only focus on avoiding or improving the cold start, there are other initialization tasks that could affect application performance. One example is connection establishment, which we optimize by an asynchronous preparation mechanism discussed in §4.2.3.

Another optimization we applied is for triggering components. We let the currently running compute component send a scheduling request to the scheduler trigger the next component(s) early on (with just-in-time pre-warming). The scheduler replies the location of the next component as soon as the location is chosen and before the next component’s environment is actually launched. With this optimization, when the current component finishes, it could directly send its output to the next component(s) without involving the scheduler.

## 4.2 Component Execution

Once a component is scheduled, the Scad execution system is responsible for executing it in an efficient manner and for facilitating its communication with other components. Below, we discuss how Scad executes its memory components and compute components and how it handles component communication and component triggering.

### 4.2.1 Memory Component Implementation

We design the execution of memory components to have proper isolation, runtime autoscaling, flexible scheduling, and fast startup. As shown in §2, memory consumption of serverless applications can vary dramatically for different inputs and during an application’s execution. Different from traditional disaggregated/remote memory systems, a unique need and challenge in the serverless setting is to quickly react to application resource changes by automatically and transparently adjusting the size of a memory component. To solve this, our main idea is to materialize each virtual memory component with dynamically added physical components.

**Execution of physical memory components.** Scad uses physical memory components as the unit of scheduling and

execution environment. One virtual memory component can consist of multiple physical memory components potentially on different nodes. Instead of making physical components all of the same size or of arbitrary sizes, we dynamically choose from a few configurable sizes for each physical component based on usage patterns (§4.3.1). For example, a 10 GB virtual memory component can be internally represented as ten 1 GB physical components or one 5 GB and five 1 GB ones. This gives Scad flexibility to balance performance and memory utilization.

The above design raises one challenge: Scad potentially needs to start many physical memory components for an application, and memory components for different applications need to be properly isolated. To isolate memory, one option is to place each physical memory component in its own virtualization environment (*e.g.*, a container), but such an environment would be slow to start and is unnecessary because memory components perform no computation.

Our proposal is to use an RDMA-based environment for each physical memory component. Specifically, we implement a *memory controller* on every node in the memory pool. It sits in the *executor* of the node, which is a user-space module that manages the node’s components and interacts with the scheduler. When the memory controller receives a request from the scheduler to start a new physical memory component, it launches one process to allocate memory and registers it with RDMA as a memory region (MR) in its own protection domain (PD). Afterwards, the memory controller establishes RDMA communication with other components, which will be discussed in §4.2.3.

**Auto-scale memory components.** To support large, dynamic memory space needs without the upfront commitment of peak memory usage (§2.1), Scad automatically scales up a virtual memory component in an on-demand fashion. When starting a virtual memory component, Scad first allocates and starts a physical memory component with *an initial size*, *e.g.*, 1 GB. As the application accesses more memory, Scad launches more physical components one at a time. Each of these physical components is of the same size (what we call *the incremental size*, *e.g.*, 128 MB). Scad dynamically determines these sizes based on historical memory usage pattern (§4.3.1)

#### 4.2.2 Compute Component Implementation

Two challenges separate Scad’s compute components from traditional FaaS functions: 1) compute components access data in remote memory and need efficient ways of such accesses, 2) we set no limit to how much memory or CPU a compute component can use and thus need mechanisms to auto-scale both memory and CPU of a compute component to potentially go beyond a single node.

To tackle these challenges in a transparent way, we implement our solutions in a per-component Scad runtime and a per-node compute controller. The *Scad runtime* sits in the sandbox that hosts the compute component (Docker container

in our implementation). It handles the Scad APIs for communicating, manages a local memory buffer, and performs resource and performance monitoring. The *compute controller* sits in the executor of every node that hosts compute components. It interacts with the scheduler and initiates, monitors, and terminates compute components.

**Local memory cache.** As many previous memory disaggregation works have shown, a small memory cache at the compute side could largely improve application performance [16, 29, 31, 50, 52]. Similarly, the Scad runtime transparently maintains a local cache at every compute component. The Scad runtime buffers asynchronous remote writes at the local cache and performs a remote write only when receiving the `sync` command (Figure 3) or when the local cache is full. The runtime checks the local cache for remote reads and avoids remote memory accesses if they hit the cache. Currently, Scad uses a default size of 64MB for the local cache and a cache line size of 4 KB. Future works could improve it with dynamic policies.

**Remote-memory access optimization.** As previous work has shown [50], remote-memory accesses could be optimized in a library to transparently improve performance. We also optimize remote-memory accesses in our libraries (Numpy and DataFrame), not only for performance but also for reducing memory consumption. Our overall approach is to 1) implement computation to have small working sets, 2) fetch only the working set that will be used right before they are used and store results back immediately after they are ready, 3) fetch/store data in a batched and asynchronous manner, 4) overlap the data fetching/storing with computation, and 5) avoid serialization/deserialization with direct accesses to remote data structures and zero memory copy. 1) and 2) reduce the local memory usage, while 3), 4), and 5) improve performance. For example, our implementation of the `join` operator fetches a small part of data at a time, by directly reading an offset of a DataFrame from a memory component. When it computes on them, it also initiates the fetching of the next batch of data in the background so that by the time the next batch is about to start the data is already fetched. Many of the optimizations are only available to Scad thanks to memory component’s disaggregated memory interface.

**Handling local memory pressure.** Compute components in the compute pool are intended to use little memory and are allocated a small amount (256 MB) for their local use. For compute components in the balanced pool, the available local memory is large but not unlimited. Both cases could run out of local memory during execution. However, Scad promises not to limit compute component’s memory size. To handle this case, Scad automatically increases a virtual compute component’s available memory by swapping when the container detects there is memory pressure. Our remote-memory swapping happens entirely in the user space using Linux `userfaultfd` and is transparent to user applications. Specifically, the Scad runtime uses a background thread to



monitor page faults caused by the user application threads. When a fault happens, if there is not enough swap space, the runtime asks the scheduler to create and launch a new physical memory component. The runtime’s background thread swaps out pages whenever it detects memory pressure. Since the user-space fault handler cannot access the page table and would not know the page access pattern, it uses an NRU (not-recently-used) policy by swapping out a page that has not recently been swapped in.

**Scaling compute resources.** Apart from scaling up memory resources for a compute component through swapping, Scad also supports scaling compute resources by triggering multiple parallel instances of a compute component. These parallel instances are physical compute components that are part of the original (virtual) compute component. They can access (*i.e.*, share) the same set of physical memory components that belong to a virtual memory component. We do not handle memory coherence or consistency currently and assume that they are handled by user programs or another higher-level system.

### 4.2.3 Component Communication

Unlike traditional serverless computing which involves network communication mainly when functions start/terminate, there will be more frequent, intensive communication *during* the execution of disaggregated components. In addition, more connection channels need to be established across the more fine-grained and dynamically added physical components. Thus, it is crucial to ensure that both the actual communication (data plane) and the connection set up (control plane) are fast. We propose an RDMA-based mechanism that is customized to fine-grained, serverless-style component communication.

**Control path.** The major goal of our communication control path design is to minimize network connection set up time, while allowing the direct communication between components in the data plane. When establishing an RDMA connection (*i.e.*, RDMA QP) between two nodes, they need to first exchange a set of metadata describing their own identities. Today’s RDMA systems use TCP to exchange these messages. However, two components cannot easily reach each other or establish a connection due to the dynamic and isolated nature of serverless computing. Recent RDMA-based serverless systems pre-establish RDMA connections between all the servers in a cluster [22, 63, 64], which only works with static memory regions and do not fit our dynamic launched components. Another prior work proposes to maintain a pool of containers with pre-assigned IP addresses [40]. Unlike Scad, this work still requires TCP connection to be setup when launching a function. Moreover, reusing IP addresses could break the isolation between functions. An alternative dynamic approach is to use an overlay network to enable direct communication between containers. However, our experiments show that the initialization of the overlay network takes nearly 40% of the startup time of a container. A recent work [57] enables

faster overlay network creation, but requires changes to the container runtime code.

Our idea is to leverage *non-direct but already established* connections between executors and schedulers to exchange the initial metadata message. Our observation is that a component has always established a connection with its rack-level scheduler by the time when it starts up. Moreover, the scheduler is the one that decides and thus knows the physical locations of the two components that will be communicating (*i.e.*, communicating relationship in the component graph). We let the scheduler send one side’s physical location (in the form of executor ID) to the other side’s *network virtualization module* when initiating the components. This network module sits inside the executor and only manages connection (RDMA QP) establishment. When a component wants to establish QP with another component, it sends the metadata message to the scheduler with the other component’s ID. The scheduler routes the message to target executor, which then gets sent to this other component by its network module. After both sides acquire the other’s metadata message, they establish an RDMA QP. The entire QP establishment takes only 34 ms.

To further optimize the startup performance, the QP establishment process starts as soon as the execution environment is ready, while loading user code in parallel. Doing so hides the establishment over the performance-critical path (Figure 6).

Our final idea to minimize network setup time is to reuse an RDMA QP when a component tries to establish the communication with a physical memory component located on a server that already has another physical memory component communicating with the component. Since the new and the existing physical memory components are both accessed by the same component, there is no need to isolate them and one QP is enough for both components.

**Data path.** Scad’s communication data path is based on kernel-bypassing RDMA. When a compute component calls a low-level communication API through `channel`, the Scad runtime looks up which QP it corresponds to. It then issues a one-sided RDMA operation for `read/write` memory components or a two-sided RDMA operation for `send/recv` compute components. As one virtual component can be mapped to multiple physical components, if the API call touches a memory region that is on two physical memory components, the Scad runtime dispatches two one-sided RDMA operations to these components and merge the responses. We exploit zero-copy techniques when implementing the data path to improve performance.

### 4.2.4 Component Triggering and Failure Handling

The communication between triggering components is performed only once — sending the output of a component to its subsequent component as the input. However, this one-time message is critical for failure handling, as the input that can be used for re-execution of a component after its failure.

Thus, our goal of triggering component communication is not performance but reliability.

To avoid re-executing the entire execution flow after a failure, Scad relies on recording the messages sent between triggering components via a reliable messaging system (*i.e.*, Kafka [33]). When a failure happens, we discard the crashed component and all its communicating components. We then re-execute from the persistently recorded input messages to these discarded components. This applies to memory components as well. Memory components are not durable or replicated. If a memory component crashes, all the compute components that access it (its communicating components) are discarded. If a compute component crashes, the memory components it accesses are all discarded.

Resuming from the reliably recorded messages in the above way is sufficient to guarantee *at-least-once* semantics, which is the same as today’s serverless systems [20, 54]. If no crashed component modifies external state we can further guarantee *observably exactly-once* semantics. Our failure handling design balances foreground performance and failure recovery performance compared to mechanisms that take more checkpoints [18] or those that restart the entire function chain after a failure [3, 5].

### 4.3 Component Adjustment

The final part of Scad is for component adjustment and mainly involves policies. At any single point, we want to optimize a Scad cluster to utilize resources available in different pools while improving the overall performance of all executing applications. Meanwhile, for each application, we aim to automatically adjust its resource plan based on historical usage patterns. To achieve these goals, Scad dynamically sets the default resource plan and “morphs” the component graph before the invocation of an application.

For each invocation, Scad collects resource usage for each component and reports it to the global monitor. Instead of using the metrics collected in the current invocation for component adjustment, we incorporate historical resource usages to avoid adjusting components out of one-time input changes.

#### 4.3.1 Per-component Resource Adjustment

As shown later in §5.2.4, it is critical to right-size components to hit a balance between performance and resource efficiency. To do this, Scad readjusts each component’s resource allocation periodically (*e.g.*, after every 1000 invocations). For a compute component, if the total memory usage (including swap) is below a preset threshold (256MB by default), we leave the component in the compute pool. If the swap frequency of the compute component in the compute pool is consistently high and total memory footprint exceeds this limit, Scad moves it to the balanced pool and sets its initial local memory size to the measured swap space size. For a memory component, the adjustment is its initial and incremental memory allocation sizes. We set these sizes based on

historical memory-component usage patterns.

#### 4.3.2 Component Aggregation

When disaggregated components communicate across the network, aggregating them and running them in a unified environment in the balanced pool eliminates the network communication overhead. Given all sets of communicating components and their network load profile, Scad needs to pick which sets to aggregate, as the balanced pool only has limited space that cannot fit all aggregated components. We frame this problem as a *zero-one* integer linear program (ILP) where each candidate is decided to be aggregated (1) or not (0). Each aggregation candidate is represented by its component-to-component network communication matrix, and its components’ CPU and memory usage vectors. The ILP solver assigns the binary decision variables such that the total network communication overhead is minimized (optimization function), while respecting the available resources in the balanced pool (constraint).

After aggregating two or more components, they become a new physical component that the Scad scheduler schedules. When merging a compute component with one or more memory components, we allocate one or more Scad-managed memory spaces inside the sandbox that runs the compute component code. Each such memory space represents an original memory component and is initiated to its estimated size. During execution, Scad’s runtime handles memory access calls from the compute component by memory copying to/from the local memory space. When merging  $K$  compute components, the Scad runtime starts  $K$  processes in one sandbox, each running a corresponding code piece. It handles communication API calls by sending/receiving inter-process messages. This allows Scad runtime to still monitor the communication load between the original components after aggregation.

#### 4.3.3 Component Disaggregation

When the balanced pool gets overloaded, Scad needs to disaggregate to free up resources. Determining which disaggregation candidate to choose is also done using a zero-one ILP solver. Here the goal is to incur minimum increase in network communication overhead (optimization function), while respecting the resources available in memory and compute pools (hard constraints) and freeing up a minimum amount of resources from the balanced pool (soft constraint). Note that our aggregation mechanism discussed above is what enables us to still capture the communication load between components after they are aggregated.

## 5 Evaluation

We implemented Scad on top of Apache OpenWhisk [4]. In total, Scad includes  $\sim$ 15K SLOC: 8K lines of Scala to extend Openwhisk’s scheduler and executor, and 4K lines of C together with 1.8K lines of Python for runtime and libraries. We evaluated Scad on a local cluster of 8 servers, each of which is a Dell PowerEdge R740 equipped with an Intel Xeon Gold 5128 CPU, 64 GB of memory, and a 100 Gbps Mellanox

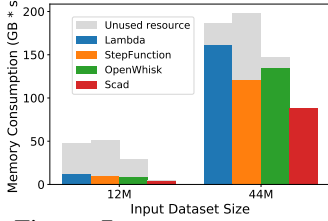


Figure 7: Memory Consumption for LR.

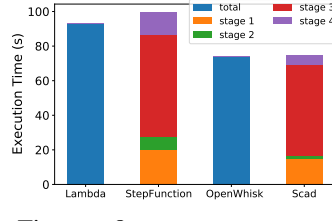


Figure 8: Execution Time Breakdown for LR.

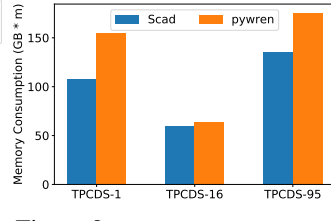


Figure 9: Memory consumption of TPC-DS.

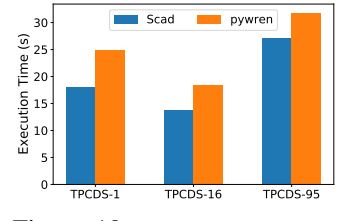


Figure 10: Execution Time of TPC-DS.

Connect-X5 NIC. All the servers are connected to a 100 Gbps FS N8560-32C 32-port switch. All servers run Ubuntu v20.04 with Linux v5.4.0. We use Docker v20.10.6 for containers.

We compare Scad with vanilla OpenWhisk [4] (running on our local cluster), AWS Lambda, AWS Step Functions [5] using Redis and S3 as intermediate storage, Azure Functions, and Pywren [34] running locally and with AWS Lambda.

## 5.1 Applications

We first present the results of running two applications on Scad and other systems in comparison.

### 5.1.1 Logistic Regression (LR) Training

Our first application is a machine learning training task using logistic regression (LR) ported from Cirrus [19]. It first loads the input data set and separates it into a training set and a validation set. Then it performs the regression on the training set. Finally, it validates the trained model with a validation set. We annotate the original code with 3 `@split` annotation points. The compiler then generates a graph of four compute components (loading, data-set splitting, training, and validation) and three memory components (training set, validation set, and learned weights).

Figure 7 plots the memory consumption using the original LR program as a whole running on AWS Lambda and OpenWhisk, our component graph running on Scad, and the same code/data split running on AWS Step Functions. We use two input dataset sizes, 12 MB and 44 MB. For Step Functions, we run one stage as one function and store the intermediate data across these stages on Redis running as an AWS t3.medium instance. All settings use the same number of vCPUs. For Lambda and OpenWhisk, we use the minimal memory that is needed to run the whole workload (2 GB). For Step Functions, we use the minimal that is needed to run each phase (2 GB, 1 GB, 2 GB, and 1 GB). Scad has minimal resource consumption and achieves over 94% resource utilization. Executing the entire program as a whole on AWS and OpenWhisk consumes more resources. Surprisingly, executing the split functions on AWS Step Functions yield more resource waste than Lambda. Even though the second and the fourth functions in the Step Functions DAG provision half of the memory, extra memory spent on load and store data to Redis in each step results in longer execution time. Memory in the container is largely wasted during this time.

Figure 8 plots the execution time of LR with the above settings. Note that since we use the same amount of vCPUs across all settings, their CPU consumption directly translates to their total execution time and we omit the presentation of CPU consumption; we do the same for other results presented. Compared to running LR as one function on OpenWhisk, splitting it to seven components on Scad introduces negligible performance overhead. In comparison, running the split stages on Step Functions introduces higher overhead compared to running one function on Lambda, mainly because of the higher communication overhead that each stage incurs.

### 5.1.2 Distributed Queries with TPC-DS

The second application we evaluate is distributed data analytics ported from the PyWren implementation of the TPC-DS benchmark [45]. PyWren splits each TPC-DS query into several stages, each containing some DataFrame operators. For each stage, PyWren generates different amount of workers to perform the computation. Each worker fetches the data to be accessed from an intermediate storage layer (Redis in our evaluation) before the computation starts and stores the data back after it finishes.

To port this application, we use the Scad DataFrame compiler and library (§3.2) to convert DataFrame operators into compute components and accessed DataFrame objects into memory components. Since with our library, DataFrame operators can directly access remote memory as computation progresses, we remove the explicit data fetching/storing steps in Pywren (except for the first and the last operator which still loads/stores data from Redis which hosts the original database).

We use a database size of 100 GB and evaluated three TPC-DS workloads with different performance characteristics and varying resource requirements: queries 1, 16, and 95. They read 2.5 GB, 20 GB, and 19 GB of data respectively and use 6 to 8 compute components and 4 to 6 memory components.

**Resource consumption and performance.** Figure 9 plots the total memory consumption of Scad and PyWren. For queries 1 and 95, Scad reduces memory consumption over PyWren for two reasons. First, different operators in a stage need different amounts of memory. With FaaS, Pywren has to provision for the peak memory (2 GB in these cases), while Scad autoscales the memory component sizes to closely follow the dynamic needs. Second, OpenWhisk pays for  $2\times$  memory

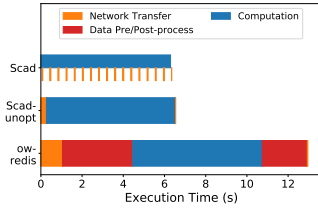


Figure 11: Runtime Breakdown of Reduce-By-Key Op.

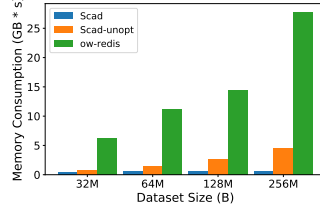


Figure 12: Memory Consumption when Scaling Input Size.

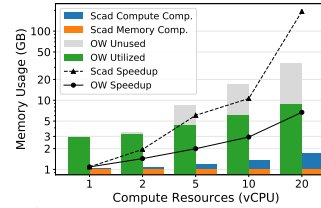


Figure 13: Memory Usage (Log Scale) and Execution Time of Reduce-By Op.

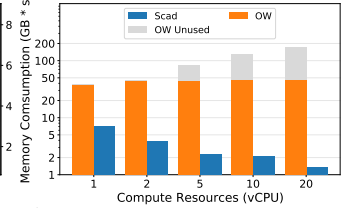


Figure 14: Memory Consumption (Log Scale) when scaling compute cores.

space when it fetches the entire dataset to the local node and has the same dataset in Redis. Scad only fetches the data that is needed for a short phase of computation *at the time when it is needed*. We further optimize memory consumption with our zero memory copy design. For Query 16, Scad and Pywren consume similar amounts of memory. The majority of this query’s execution time is on its first operator. For the first operator, both Scad and Pywren fetch the initial data from the Redis database and thus consume similar memory amounts.

Figure 10 plots the total run time of the three queries. Scad improves performance over PyWren by 15% to 28%.

**Closer look at performance.** To further understand Scad’s performance gain, we take a closer look at the 4th stage (Reduce-By-Key) in Query 1. Figure 11 shows the latency breakdown time line of the execution this stage (excluding container environment startup time). OpenWhisk’s performance is much worse than Scad mainly because of its data pre- and post-processing, including serialization, data-set partitioning, and de-serialization. In contrast, Scad’s disaggregation uses a memory model to directly read/write remote memory into/from local data structures, without the need for any serialization or memory copying. Scad’s RDMA-based network also contributes to faster network transfer. Finally, Scad’s library optimization (§4.2.2) further improves the performance by reading/writing remote memory in an asynchronous and batched manner, effectively hiding almost all the network communication and setup overhead behind foreground computation.

**Independent scaling of compute and memory.** To demonstrate Scad’s ability to independently scale compute and memory resources, we take a closer look at the Reduce-By-Key stage. Figure 12 plots the memory consumption of computational function when we change the input dataset size, while fixing the compute resources to 20 vCPUs. When input data size increases from 64 MB to 1 GB, Scad’s memory size increases by 1.1 GB, while OpenWhisk’s increases by 3.6 GB. Both systems can use different amounts of memory with the same number of vCPUs (*i.e.*, scaling memory without scaling compute). OpenWhisk’s memory consumption is higher than Scad because OpenWhisk requires more memory and execution time to load/store data for each function, and the loaded data occupies memory for the entire duration of a function. Scad directly accesses data in memory nodes at the time when the data is needed.

We then evaluate Scad’s ability to independently scale compute resources (when fixing the input data to 1 GB). Figure 13 plots the memory usage and run-time speedup when increasing compute resources (in vCPUs). To model today’s public cloud serverless offerings, we set each OpenWhisk function’s CPU and memory to have a fixed ratio (*i.e.*, 1 vCPU and 1,769 MB memory, which is the same as the ratio used in AWS Lambda). OpenWhisk scales out by triggering more parallel instances of a function. Because of the fixed-coupling of CPU and memory, this scaling results in  $20\times$  provisioned memory when amount of vCPUs increases by  $20\times$ . In contrast, Scad scales only its compute component by invoking 1 to 20 instances of it, while using the same number of memory components. As a result, Scad’s total memory size only increases by 67.4% when its CPU resources increase by  $20\times$ . For OpenWhisk, in addition to provisioned memory size, we also measure the amount of memory that is used during function execution. Its used memory increases by  $2.05\times$ , which is much lower than the  $20\times$  increase in its provisioned memory. This is because the total amount of data to be processed is the same when scaling out, and we shard the data across all the functions, resulting in each processing only a shard. Worth noticing is that even when removing the fixed-ratio limitation, OpenWhisk’s used memory is still much higher than Scad’s total memory ( $2.05\times$  vs. 67.4%). This is because OpenWhisk requires extra memory in each function for data loading (*e.g.*, data structures for serialization/de-serialization).

Scad also achieves a much higher speedup than OpenWhisk when scaling out, because it avoids function performance overheads such as serialization and data partitioning. Because of the high speedup and minimal memory consumption, Scad’s total memory consumption (GB $\times$ min) *decreases* by 81% when scaling up, while OpenWhisk’s provisioned memory increased by 4.57x, and used memory increased by 21.6% as shown in Figure 14.

## 5.2 Micro-benchmarks

To further understand Scad and compare it with other systems, we performed a set of additional evaluations using micro-benchmarks.

### 5.2.1 Component Elasticity

**Auto-scaled memory components.** To demonstrate how Scad dynamically scales memory, we build a simple workload inspired by the video processing example in §2.1. It loads a

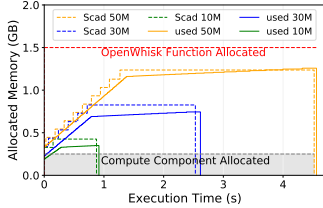


**Figure 15: Memory Elasticity.** For three different input size. Dashed lines for Scad include memory allocated on both memory components and compute components.

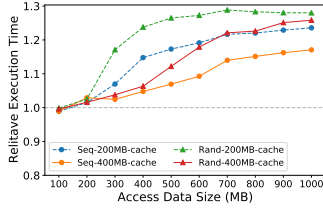


**Figure 16: Elastic Compute.** With different local memory size.

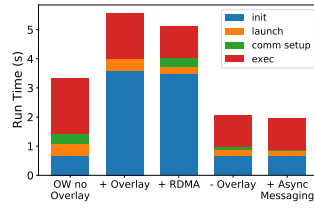


**Figure 17: Effect of Scad's Techniques on Run Time.**

System Config	Time
OpenWhisk	773 ms
OpenWhisk + Overlay	1188 ms
Scad + Overlay	1002 ms
Scad no pre-warm	595 ms
Full Scad (pre-warm)	284 ms
AWS Lambda	140 ms
AWS Step Functions	215 ms
Azure Durable Functions	270 ms

**Table 1: Application Cold Start Time.**

compressed DataFrame dataset, performs random sampling on the dataset, and returns the sampling results. Figure 15 shows the amount of memory actually used by the workload and memory allocated by Scad. When calculating Scad's memory consumption, we also include the local memory used by compute components, which is a fixed but small amount (shown at the bottom of the figure). Scad closely follows the real memory usage by adding more physical memory components as memory usages increase. In contrast, OpenWhisk (and public clouds like AWS) can only set containers at a few fixed memory sizes and provision for the peak usage. In this case, the nearest OpenWhisk can provision is 1.5 GB.

### Auto-scaled compute components with memory swapping

Scad automatically and transparently scales a compute component up with memory swapping when the component is low on memory. To measure our swap system performance, we use a simple microbenchmark of sequentially or randomly reading an array that is configured to be from 100 MB to 1000 MB. Figure 16 plots the total run time of the microbenchmark with increasing array size. We test two local cache sizes: 200 MB and 400 MB, and compare the swap performance against the case where the local memory is larger than the whole array size (*i.e.*, no swapping and the ideal performance but impossible with the compute pool configuration). Overall, swapping adds 1% to 26% performance overhead. The overhead is higher when the array size is bigger and when the local memory size is smaller.

### 5.2.2 Component Execution

To understand the impact of various Scad techniques on application performance, we run a graph with one compute component that access one memory component. Figure 17 demonstrates the effect as we add more techniques to the baseline. The first bar is the baseline OpenWhisk without an overlay network (and thus cannot support dynamic component-to-component communicate). The second bar adds the overlay network (so that components can directly communicate with each other); the overlay network increases the initialization time. The third bar BS the TCP stack in the second bar with our RDMA stack, which improves the component execution time but also adds a small communication set up time. The fourth bar removes the overlay network and uses our network virtualization module, which reduces the initialization time.

The final bar includes our asynchronous messaging optimization and hides the network connection setup time.

### 5.2.3 Component Launching and Scheduling

**Cold start performance.** To measure cold start performance, we created an application graph with 10 distinct compute components in a chain, each sleeping for 100 ms. We launched the application and measured the end-to-end latency across a variety of systems. For each system, we calculate the average cold start overhead per component over 20 trails. Table 1 shows the cold start time. All the rows except for Azure and AWS run on our local cluster. Similar to Figure 17, the overlay network adds significant overhead to the startup time for both OpenWhisk and Scad. Scad's just-in-time pre-warming mechanism further reduces the cold start time to 72%. Azure and AWS in general have better cold start performance, mainly because of their lightweight sandboxing mechanisms like Firecracker [13], while OpenWhisk and Scad use Docker, which is much slower to start up. Optimizing sandboxes for serverless computing has been well studied and is out of scope for this paper.

**Warm start performance.** Figure 18 measures the warm start performance in a similar way as our cold start experiment, over 20 trials. For this experiment, we warm up all the functions/components in the workload. We vary the per-compute-component execution code (sleep for 10ms, 100ms, or 1000ms). Scad's warm start time improves by more than 90% improvement over AWS Step Function and 70% over OpenWhisk. This is due to Scad's scheduling mechanism that moves scheduling ]off the critical path.

**Locality-aware scheduling.** Scad's locality-aware scheduling aims to put communicating components as close to each other as possible before resorting to aggregation. Figure 19 demonstrates the effect of our scheduling and puts it in perspective with running OpenWhisk and Redis on our local cluster and running on AWS Lambda with S3. We also evaluate Scad without using the locality-aware scheduling (Scad\_nolocal). For this setting, we assign all memory component to a single executor. The workload launches 1 to 50 compute-memory-component pairs. Since Scad always try to put communicating components (a compute-memory pair) on the same server, its aggregated communication throughput is much higher and the average latency is lower than all other

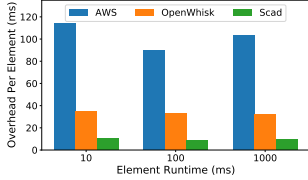


Figure 18: Application Warm Start Overhead.

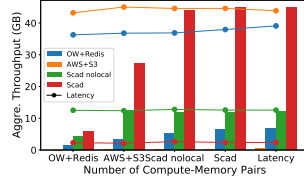


Figure 19: Effect of Scad Locality Scheduling.

schemes. Scad also scales better than Redis and Scad\_nolocal by utilizing local network bandwidth. As expected, S3’s performance is the worst.

**Scheduler Scalability** We evaluated the maximum throughput of Scad’s rack-level scheduler and found that it can handle around 20K scheduling requests per second. This scheduling rate is similar to OpenWhisk’s scheduler. However, thanks to our locality based design with a scheduler-per-rack, the number of total messages that the system can handle scales linearly with the number of racks. We also find the request rate to the top-level scheduler to be light (around 50K requests per second) and is never the bottleneck in the system.

## 5.2.4 Component Adjustment

**Single-component adjustment.** We evaluate the effect of our dynamic adjustment of the initial and incremental memory component sizes (§4.3.1) using real-world serverless application memory usage profiles from Azure [51]. This dataset contains a set of real-world applications, each being invoked many times with different user inputs. In addition to using the average memory pattern from this dataset, we further choose a few representative applications to highlight. Figure 20 plots the CDF of memory usage across invocations of these representative applications and the average memory usage of all applications in the trace. The representative applications are *Small*: most invocations’ memory usages are small, *Large*: most invocations used a lot of memory, and *Varying*: different invocations’ memory usages vary largely. For comparison, we also plot a straight line of 256 MB, which is the default initial memory allocation size in Scad.

Figure 21 plots the performance and memory utilization with three schemes: fixing initial and incremental sizes to 256 MB and 64 MB, provision memory components to the highest usage (peak-provision), and our dynamic adjustment policy. Overall, our dynamic policy is Pareto optimal (high utilization and good performance). Peak provisioning achieves the best performance, since no auto-scaling or swapping will be incurred. But its memory utilization is low. A fixed configuration can lead to both poor resource utilization (when real usage is below the configuration) and poor performance (when frequently adding many physical memory components at runtime).

**Component aggregation and disaggregation.** To demonstrate our disaggregation and aggregation policy as discussed in §4.3, we run three applications concurrently on our cluster configured with a memory pool, a compute pool, and a

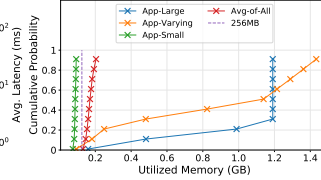


Figure 20: Sampled Memory Utilization of Functions.

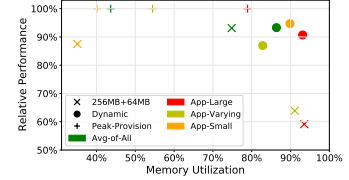


Figure 21: Resource Adjustment. More top-right is better.

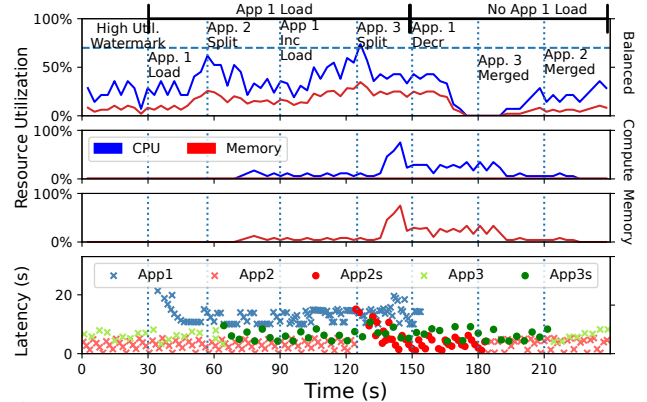


Figure 22: Timeline of Pool Utilization and Application Performance. Crosses represent aggregated execution. Dots represent disaggregated execution (App2s and App3s).

balanced pool, as shown in Figure 22. App1 is a compute component that cannot be disaggregated. App2 and App3 each has a compute and a memory component that can either be aggregated or disaggregated. Communication between App3’s components is much higher than App2’s. At  $t = 0$ , App2 and App3 are invoked at steady rate as warmed, aggregated components. As we trigger invocations of App1 from  $t = 30$  to  $t = 150$ , the utilization of the balanced pool reaches the high utilization watermark (70% in this experiment), and Scad’s disaggregation policy gets triggered at  $t = 63$ . It decides to disaggregate App2 first since based on history, it has a lower communication load than App3. Doing so is enough to bring the utilization beneath the watermark. As App1’s invocation rate continues to rise, at  $t = 117$ , the disaggregation policy gets triggered again and Scad chooses to disaggregate App3. The invocation rate of App1 decreases from  $t = 150$  to  $t = 240$ , which frees up space in the balanced pool. As a result, our policy decides to aggregate App3 and then App2.

Aggregation improves performance of App2 by 26% and App3 by 5%. Running both applications in an aggregated fashion (§4.3.2) have only less than 2% performance overhead compared to a non-split version of the programs (original programs without any code split). Note that we artificially make App2 to be extremely communication-intensive, which is rare in reality. Aggregating other applications shows an average performance improvement of 14%.

## 6 Discussion and Future Work

**Supporting non-CPU-memory resources.** Although Scad currently only supports the disaggregation and aggregation of CPU and memory resources, the general concept of resource-

centric serverless computing via disaggregation and aggregation could apply to other types of resources, such as accelerators and non-DRAM storage media. For example, applications that can benefit from hardware-acceleration would want to run some of their computation on GPU, FPGA, or an ASIC. Applications that desire low-cost data storage options may want to place some data components in persistent memory or flash. To integrate these heterogeneous hardware resources, one needs to first be able to disaggregate them over the network. Some recent works have shown the promise of disaggregating heterogeneous hardware, with solutions like GPU-direct [43], rCUDA [25], disaggregated flash [36], and SmartNIC-driven accelerator [58]. Apart from disaggregation, isolated execution environments need to be established on each disaggregated node, together with a module that can assist with network connection setup. Finally, we can extend our low-level and high-level APIs to support the added hardware type (e.g., by annotating a function to be executed in GPU) and use existing compilers to compile user code to the hardware if needed.

**Compiler and profiling extension.** Scad’s current frontend requires programmer input or domain information (e.g., DataFrame operators) as the criteria for identifying resource components. These information can be inaccurate or imprecise, and getting it requires some programmer effort. To capture resource changes in an application more precisely and automatically, future works could capture real resource usages from either a *dry run* of the program or *sampled* real runs. For example, tools like Scalene [9], pprofile [8], and Memray [10] could capture fine-grained (e.g., line-by-line) CPU and memory usages of Python programs. Before deploying a program to the cloud, users could perform a dry run with sample anticipated input data and capture resource usages. They can then add `@split` annotations to where the resource usages dramatically change. This annotated code will then be the initial deployed version of the application. After deployment, the cloud system can also sample a few real runs to perform a similar profiling and *re-compilation* process (e.g., with Profiling-Guided Optimization or PGO) to produce new component graphs that can better capture the resource usage patterns with real user inputs.

**Disaggregation architectures.** The current implementation and evaluation of Scad are on server-based disaggregation clusters. The general Scad design can be generalized to other disaggregated architecture such as hardware-based disaggregated devices and interconnects like Ethernet and CXL. A recent work [32] builds an Ethernet-based hardware disaggregated memory device. To support Scad, we can let compute node’s controller use Clio’s remote memory allocation and address-space-based protection to create physical memory components, similar to our current RDMA-based allocation and protection domain. We also need to change the network virtualization module to work with Clio’s network communication mechanism. We believe that a similar approach like the

above can be applied to other existing or future disaggregation architecture.

**Security implications.** New vulnerabilities can arise in a resource-centric serverless environment (and in a disaggregation environment in general), as resource disaggregation naturally expands the footprint of serverless applications: more out-of-server communication would take place and a higher number of servers would be touched to host resources required for the same application. For example, there can be direct and side channels to steal information from messages sent over the network. Malicious users could also launch Denial-of-Service attacks to overload a memory node (or even an entire pool). We believe many traditional security measures can be devised or adapted for a disaggregated environment. Devising attacks and mitigations are both beyond the scope of this paper and are left for future work.

## 7 Conclusion

We present Scad, a resource-centric serverless computing framework based on the ideas of resource disaggregation and aggregation. We show that disaggregation can be used to lift the limits of current serverless platforms while still maintaining comparable or even better performance. Our evaluation of Scad demonstrates its benefits in resource saving and performance improvement.

## References

- [1] tibanna Documentation. Technical report, Tibanna, April 2021. [https://tibanna.readthedocs.io/\\_/downloads/en/latest/pdf/](https://tibanna.readthedocs.io/_/downloads/en/latest/pdf/).
- [2] Using Driverless AI. Technical report, H2O.ai, April 2021. <http://docs.h2o.ai/driverless-ai/latest-stable/docs/userguide/UsingDriverlessAI.pdf>.
- [3] Apache OpenWhisk Composer, Accessed 2022-04-16. <https://github.com/apache/openwhisk-composer>.
- [4] Apache OpenWhisk: Open source serverless cloud platform, Accessed 2022-04-16. <https://openwhisk.apache.org/>.
- [5] AWS Step Functions, Accessed 2022-04-16. <https://aws.amazon.com/step-functions/>.
- [6] Azure Durable Functions, Accessed 2022-04-16. <https://azure.microsoft.com/en-us/pricing/details/functions/>.
- [7] Azure Functions Pricing, Accessed 2022-04-16. <https://azure.microsoft.com/en-us/pricing/details/functions/>.
- [8] pprofile: Line-granularity, thread-aware deterministic and statistic pure-python profiler, Accessed 2022-04-16. <https://github.com/vpelletier/pprofile>.
- [9] Scalene: a high-performance CPU, GPU and memory profiler for Python, Accessed 2022-04-16. <https://github.com/plasma-umass/scalene>.

- [10] Memray, Accessed 2022-04-20. <https://github.com/bloomberg/memray>.
- [11] Cristina Abad, Ian T. Foster, Nikolas Herbst, and Alexandru Iosup. Serverless Computing (Dagstuhl Seminar 21201). *Dagstuhl Reports*, 11(4):34–93, 2021.
- [12] Jason Adrian. Introducing Bryce Canyon: Our next-generation storage platform, Accessed 2022-04-16. <https://code.fb.com/data-center-engineering/introducing-bryce-our-next-generation-storage-platform/>.
- [13] Alexandru Agache, Marc Brooker, Alexandra Iordache, Anthony Liguori, Rolf Neugebauer, Phil Piwonka, and Diana-Maria Popa. Firecracker: Lightweight Virtualization for Serverless Applications. In *17th USENIX Symposium on Networked Systems Design and Implementation (NSDI '20)*, Santa Clara, CA, February 2020.
- [14] Istemi Ekin Akkus, Ruichuan Chen, Ivica Rimac, Manuel Stein, Klaus Satzke, Andre Beck, Paarijaat Aditya, and Volker Hilt. SAND: Towards high-performance serverless computing. In *2018 USENIX Annual Technical Conference (ATC '18)*, July 2018.
- [15] Alibaba Cloud. Super computing cluster, Accessed 2022-04-16. <https://www.alibabacloud.com/product/scc>.
- [16] Emmanuel Amaro, Christopher Branner-Augmon, Zhihong Luo, Amy Ousterhout, Marcos K. Aguilera, Aurojit Panda, Sylvia Ratnasamy, and Scott Shenker. Can far memory improve job throughput? In *Proceedings of the Fifteenth European Conference on Computer Systems (EuroSys '20)*, New York, NY, April 2020.
- [17] Muhammad Bilal, Marco Canini, Rodrigo Fonseca, and Rodrigo Rodrigues. With great freedom comes great opportunity: Rethinking resource allocation for serverless functions. *arXiv preprint arXiv:2105.14845*, 2021.
- [18] Sebastian Burckhardt, Chris Gillum, David Justo, Konstantinos Kallas, Connor McMahon, and Christopher S. Meiklejohn. Durable functions: Semantics for stateful serverless. In *Proceedings of the ACM on Programming Languages (OOPSLA '21)*, New York, NY, October 2021.
- [19] Joao Carreira, Pedro Fonseca, Alexey Tumanov, Andrew Zhang, and Randy Katz. Cirrus: A serverless framework for end-to-end ML workflows. In *Proceedings of the ACM Symposium on Cloud Computing (SoCC '19)*, November 2019.
- [20] Google Cloud. Cloud Functions execution environment - execution guarantees, Accessed 2022-04-16. <https://cloud.google.com/functions/docs/concepts/exec>.
- [21] Marcin Copik, Grzegorz Kwasniewski, Maciej Besta, Michal Podstawski, and Torsten Hoefer. SeBS: A serverless benchmark suite for function-as-a-service computing. In *Proceedings of the 22nd International Middleware Conference (Middleware '21)*, Québec city, Canada, December 2021.
- [22] Marcin Copik, Konstantin Taranov, Alexandru Calotoiu, and Torsten Hoefer. rFaaS: RDMA-enabled FaaS platform for serverless high-performance computing. *arXiv preprint arXiv:2106.13859*, 2021.
- [23] Datadog. The state of serverless, May 2021. <https://www.datadoghq.com/state-of-serverless/>.
- [24] Aleksandar Dragojević, Dushyanth Narayanan, Orion Hodson, and Miguel Castro. FaRM: Fast Remote Memory. In *Proceedings of the 11th USENIX Conference on Networked Systems Design and Implementation (NSDI '14)*, Seattle, WA, April 2014.
- [25] José Duato, Antonio J Pena, Federico Silla, Rafael Mayo, and Enrique S Quintana-Ortí. rcuda: Reducing the number of gpu-based accelerators in high performance clusters. In *2010 International Conference on High Performance Computing & Simulation (HPCS '10)*, Orlando, FL, June 2010.
- [26] Vojislav Dukic, Rodrigo Bruno, Ankit Singla, and Gustavo Alonso. Photons: Lambdas on a diet. In *Proceedings of the 11th ACM Symposium on Cloud Computing (SoCC '20)*, Virtual, October 2020.
- [27] Simon Eismann, Long Bui, Johannes Grohmann, Cristina Abad, Nikolas Herbst, and Samuel Kounev. Sizeless: Predicting the optimal size of serverless functions. In *Proceedings of the 22nd International Middleware Conference (Middleware '21)*, New York, NY, May 2021. ACM.
- [28] Alexander Fuerst and Prateek Sharma. FaaSCache: keeping serverless computing alive with greedy-dual caching. In *Proceedings of the 26th ACM International Conference on Architectural Support for Programming Languages and Operating Systems (ASPLOS '21)*, Virtual, April 2021.
- [29] Peter X. Gao, Akshay Narayan, Sagar Karandikar, Joao Carreira, Sangjin Han, Rachit Agarwal, Sylvia Ratnasamy, and Scott Shenker. Network Requirements for Resource Disaggregation. In *12th USENIX Symposium on Operating Systems Design and Implementation (OSDI '16)*, Savannah, GA, October 2016.
- [30] Pedro García-López, Aleksander Slominski, Simon Shillaker, Michael Behrendt, and Barnard Metzler. Serverless end game: Disaggregation enabling transparency. *arXiv preprint arXiv:2006.01251*, 2020.



- [31] Juncheng Gu, Youngmoon Lee, Yiwen Zhang, Mosharaf Chowdhury, and Kang Shin. Efficient Memory Disaggregation with Infiniswap. In *Proceedings of the 14th USENIX Symposium on Networked Systems Design and Implementation (NSDI '17)*, Boston, MA, April 2017.
- [32] Zhiyuan Guo, Yizhou Shan, Xuhao Luo, Yutong Huang, and Yiyang Zhang. Clio: A Hardware-Software Co-Designed Disaggregated Memory System. In *Proceedings of the 27th ACM International Conference on Architectural Support for Programming Languages and Operating Systems (ASPLOS '22)*, Lausanne, Switzerland, March 2022.
- [33] Jun Rao Jay Kreps, Neha Narkhede. Kafka: A distributed messaging system for log processing. In *Proceedings of the 6th International Workshop on Networking Meets Databases (NetDB '11)*, Athens, Greece, June 2011.
- [34] Eric Jonas, Qifan Pu, Shivaram Venkataraman, Ion Stoica, and Benjamin Recht. Occupy the cloud: Distributed computing for the 99%. In *Proceedings of the 2017 Symposium on Cloud Computing (SoCC '17)*, Santa Clara, CA, September 2017.
- [35] Anuj Kalia, Michael Kaminsky, and David G. Andersen. Using RDMA Efficiently for Key-value Services. In *Proceedings of the 2014 ACM Conference on Special Interest Group on Data Communication (SIGCOMM '14)*, Chicago, IL, USA, August 2014.
- [36] Ana Klimovic, Heiner Litz, and Christos Kozyrakis. Reflex: Remote flash == local flash. *ACM SIGARCH Computer Architecture News*, 45(1):345–359, 2017.
- [37] Ana Klimovic, Yawen Wang, Patrick Stuedi, Animesh Trivedi, Jonas Pfefferle, and Christos Kozyrakis. Pocket: Elastic ephemeral storage for serverless analytics. In *13th USENIX Symposium on Operating Systems Design and Implementation (OSDI '18)*, Carlsbad, CA, October 2018.
- [38] AWS Lambda. Configuring Lambda function memory, Accessed 2021-12-13. <https://docs.aws.amazon.com/lambda/latest/dg/configuration-memory.html>.
- [39] Zijun Li, Yushi Liu, Linsong Guo, Quan Chen, Jiagan Cheng, Wenli Zheng, and Minyi Guo. Faasflow: enable efficient workflow execution for function-as-a-service. In *Proceedings of the 27th ACM International Conference on Architectural Support for Programming Languages and Operating Systems (ASPLOS '22)*, Lausanne, Switzerland, March 2022.
- [40] Anup Mohan, Harshad Sane, Kshitij Doshi, Saikrishna Edupuganti, Naren Nayak, and Vadim Sukhominov. Agile cold starts for scalable serverless. In *11th USENIX Workshop on Hot Topics in Cloud Computing (HotCloud '19)*, Renton, WA, July 2019.
- [41] Djob Mvondo, Mathieu Bacou, Kevin Nguetchouang, Lucien Ngale, Stéphane Pouget, Josiane Kouam, Renaud Lachaize, Jinho Hwang, Tim Wood, Daniel Hagimont, et al. OFC: an opportunistic caching system for FaaS platforms. In *Proceedings of the Sixteenth European Conference on Computer Systems (EuroSys '21)*, Virtual, April 2021.
- [42] Jacob Nelson, Brandon Holt, Brandon Myers, Preston Briggs, Luis Ceze, Simon Kahan, and Mark Oskin. Latency-Tolerant software distributed shared memory. In *2015 USENIX Annual Technical Conference (ATC '15)*, Santa Clara, CA, July 2015.
- [43] NVIDIA. NVIDIA GPUDirect. <https://developer.nvidia.com/gpudirect>, 2010.
- [44] Nathan Pemberton and Johann Schleier-Smith. The serverless data center: Hardware disaggregation meets serverless computing. In *The First Workshop on Resource Disaggregation (WORD '19)*, Providence, RI, April 2019.
- [45] Meikel Poess, Bryan Smith, Lubor Kollar, and Paul Larson. Tpc-ds, taking decision support benchmarking to the next level. In *Proceedings of the 2002 ACM SIGMOD international conference on Management of data (SIGMOD '02)*, Madison, Wisconsin, June 2002.
- [46] Qifan Pu, Shivaram Venkataraman, and Ion Stoica. Shuffling, fast and slow: Scalable analytics on serverless infrastructure. In *16th USENIX Symposium on Networked Systems Design and Implementation (NSDI '19)*, Boston, MA, February 2019.
- [47] Matthew Rocklin. Dask: Parallel computation with blocked algorithms and task scheduling. In *Proceedings of the 14th python in science conference (SciPy '15)*, Austin, TX, July 2015.
- [48] Francisco Romero, Gohar Irfan Chaudhry, Íñigo Goiri, Pragna Gopa, Paul Batum, Neeraja J. Yadwadkar, Rodrigo Fonseca, Christos Kozyrakis, and Ricardo Bianchini. FaaS\$T: A transparent auto-scaling cache for serverless applications. In *Proceedings of the ACM Symposium on Cloud Computing (SoCC '21)*, New York, NY, November 2021.
- [49] Rohan Basu Roy, Tirthak Patel, and Devesh Tiwari. Ice-Breaker: Warming serverless functions better with heterogeneity. In *Proceedings of the 27th ACM International Conference on Architectural Support for Programming Languages and Operating Systems (ASPLOS '22)*, Lausanne, Switzerland, April 2022.

- [50] Zhenyuan Ruan, Malte Schwarzkopf, Marcos K. Aguilera, and Adam Belay. AIFM: High-Performance, Application-Integrated Far Memory. In *14th USENIX Symposium on Operating Systems Design and Implementation (OSDI '20)*, Banff, Canada, November 2020.
- [51] Mohammad Shahradd, Rodrigo Fonseca, Íñigo Goiri, Gohar Chaudhry, Paul Batum, Jason Cooke, Eduardo Laureano, Colby Tresness, Mark Russinovich, and Ricardo Bianchini. Serverless in the wild: Characterizing and optimizing the serverless workload at a large cloud provider. In *2020 USENIX Annual Technical Conference (ATC '20)*, Virtual, July 2020.
- [52] Yizhou Shan, Yutong Huang, Yilun Chen, and Yiying Zhang. LegoOS: A Disseminated, Distributed OS for Hardware Resource Disaggregation. In *Proceedings of the 13th USENIX Symposium on Operating Systems Design and Implementation (OSDI '18)*, Carlsbad, CA, October 2018.
- [53] Simon Shillaker and Peter Pietzuch. FAASM: lightweight isolation for efficient stateful serverless computing. In *2020 USENIX Annual Technical Conference (ATC '20)*, Virtual, July 2020.
- [54] Craig Shoemaker, Jeff Hollan, David Coulter, Daniel Cazzulino, Alex Mang, Andy J, and Glenn Gailey. Azure Functions reliable event processing, May 2020. <https://docs.microsoft.com/en-us/azure/azure-functions/functions-reliable-event-processing>.
- [55] Arjun Singhvi, Arjun Balasubramanian, Kevin Houck, Mohammed Danish Shaikh, Shivaram Venkataraman, and Aditya Akella. Atoll: A scalable low-latency serverless platform. In *Proceedings of the ACM Symposium on Cloud Computing (SoCC '21)*, Seattle, WA, November 2021.
- [56] Vikram Sreekanti, Chenggang Wu, Xiayue Charles Lin, Johann Schleier-Smith, Joseph E Gonzalez, Joseph M Hellerstein, and Alexey Tumanov. Cloudburst: Stateful functions-as-a-service. In *Proceedings of the VLDB Endowment (VLDB '20)*, Tokyo, Japan, August 2020.
- [57] Shelby Thomas, Lixiang Ao, Geoffrey M. Voelker, and George Porter. Particle: Ephemeral endpoints for serverless networking. In *Proceedings of the 11th ACM Symposium on Cloud Computing (SoCC '20)*, New York, NY, October 2020.
- [58] Maroun Tork, Lina Maudlej, and Mark Silberstein. Lynx: A smartnic-driven accelerator-centric architecture for network servers. In *Proceedings of the Twenty-Fifth International Conference on Architectural Support for Programming Languages and Operating Systems (ASPLOS '20)*, Lausanne, Switzerland, March 2020.
- [59] Shin-Yeh Tsai, Yizhou Shan, , and Yiying Zhang. Disaggregating Persistent Memory and Controlling Them from Remote: An Exploration of Passive Disaggregated Key-Value Stores. In *Proceedings of the 2020 USENIX Annual Technical Conference (ATC '20)*, Boston, MA, USA, July 2020.
- [60] Francisco Javier Vera-Olmos, Esteban Pardo, Helena Melero, and Norberto Malpica. Deepeye: Deep convolutional network for pupil detection in real environments. *Integrated Computer-Aided Engineering*, 26(1):85–95, 2019.
- [61] Ao Wang, Jingyuan Zhang, Xiaolong Ma, Ali Anwar, Lukas Rupperecht, Dimitrios Skourtis, Vasily Tarasov, Feng Yan, and Yue Cheng. InfiniCache: Exploiting ephemeral serverless functions to build a cost-effective memory cache. In *18th USENIX Conference on File and Storage Technologies (FAST '20)*, Santa Clara, CA, February 2020.
- [62] Chenxi Wang, Haoran Ma, Shi Liu, Yuanqi Li, Zhenyuan Ruan, Khanh Nguyen, Michael D. Bond, Ravi Ne-travali, Miryung Kim, and Guoqing Harry Xu. Semeru: A memory-disaggregated managed runtime. In *14th USENIX Symposium on Operating Systems Design and Implementation (OSDI '20)*, Banff, Canada, November 2020.
- [63] Xingda Wei, Fangming Lu, Rong Chen, and Haibo Chen. Krcore: a microsecond-scale rdma control plane for elastic computing. *arXiv preprint arXiv:2201.11578*, 2021.
- [64] Xingda Wei, Tianxia Wang, Jinyu Gu, Yuhan Yang, Fangming Lu, Rong Chen, and Haibo Chen. Booting 10k serverless functions within one second via RDMA-based remote fork. *arXiv preprint arXiv:2203.10225*, 2022.
- [65] Wes McKinney. Data Structures for Statistical Computing in Python. In *Proceedings of the 9th Python in Science Conference (SciPy '10)*, Austin, Texas, June 2010.
- [66] Fei Xu, Yiling Qin, Li Chen, Zhi Zhou, and Fangming Liu.  $\lambda$ dnn: Achieving predictable distributed dnn training with serverless architectures. *IEEE Transactions on Computers*, 71(2):450–463, 2021.
- [67] Wen Zhang, Vivian Fang, Aurojit Panda, and Scott Shenker. Kappa: a programming framework for serverless computing. In *Proceedings of the 11th ACM Symposium on Cloud Computing (SoCC '20)*, Virtual, October 2020.